

Article

Cumulative Effect of Strength Enhancer—Lanthanum and Ductility Enhancer—Cerium on Mechanical Response of Magnesium

Wei Yang , Sravya Tekumalla *  and Manoj Gupta *

Department of Mechanical Engineering, National University of Singapore, Singapore 117576, Singapore; a0119386@u.nus.edu

* Correspondence: tvrlsravya@u.nus.edu (S.T.); mpegm@nus.edu.sg (M.G.); Tel.: +65-6516-6358 (S.T. & M.G.)

Received: 2 June 2017; Accepted: 26 June 2017; Published: 29 June 2017

Abstract: In the present work, the cumulative effect of strength enhancer Lanthanum (La) and ductility enhancer Cerium (Ce) on the mechanical response of pure Mg was investigated. A ternary Mg-4La-0.4Ce alloy was developed using a disintegrated melt deposition method followed by hot extrusion. The mechanical characterization revealed that the ternary alloy exhibited superior hardness and tensile and compressive strengths when compared to Mg and Mg-0.4Ce binary alloy, thereby validating the role of La as a strength enhancer. Furthermore, the ductility of the chosen alloy was also enhanced as compared to Mg and other La rich Mg alloys, indicating that the ductility enhancement is primarily due to Ce. The microstructural characterization revealed that the cumulative addition of La and Ce refined the grain size and led to the formation of a large volume of secondary phases which affected the mechanical properties. The effect of fine grains and the presence of secondary phases on the deformation behavior of the alloy were conclusively ascertained with the aid of deformation and fracture studies.

Keywords: magnesium; Mg-4La-0.4Ce alloy; extrusion; strength; ductility and microstructure

1. Introduction

Being the lightest structural metal with a relatively high specific strength, magnesium (Mg) can be used to improve fuel and system efficiency through weight reduction. Mg, with a hexagonal close-packed structure, consists of three slip systems including basal, prismatic and pyramidal slip [1]; however, the critical resolved shear stress (CRSS) is too high for non-basal slip to occur at room temperature. Thus, with only two independent basal slip systems, its ductility and formability are poor. After secondary processing like extrusion, Mg develops and exhibits a strong basal texture which further limits its ductility. In order to weaken the basal texture and improve room temperature ductility, Mg is alloyed with Rare Earth (RE) elements to facilitate both non-basal slip and cross-slip of screw dislocations [2]. This altered texture, RE texture component, has $\langle 11\bar{2}1 \rangle$ direction parallel to the extrusion direction [3]. This alignment also favors non-basal slip in the extrusion direction, which is the reason for the improved ductility. Mg-Ce based alloys demonstrate some beneficial characteristics in terms of absolute strength, elongation to failure and a relatively better yield symmetry in exhibiting texture randomization. An investigation by Mishra et al. reported an increased ductility through the addition of 0.2 wt. % Ce to Mg while its yield strength was compromised [4]. The results were attributed to an altered texture during dynamic recrystallization through alignment of the c-axis of the grains to a direction which favors non-basal slip, as well as an increase in the stacking fault energy which promotes cross slips [5]. In another investigation, by adopting the Disintegrated Melt Deposition (DMD) technique followed by extrusion, Tekumalla et al. [6] obtained the as-extruded Mg-0.4Ce alloy

with excellent overall mechanical properties including an improvement in tensile yield strength by 182%, as compared to pure Mg and a tensile ductility of 27%.

The strengthening mechanisms in Mg alloys with RE elements include grain-boundary strengthening, solid solution strengthening and precipitation strengthening, depending on the type and amount of RE element addition. For the case of La, the solubility in Mg is very limited, and hence, the formation of intermetallics is inevitable [7]. Depending on the concentration of solute, the intermetallics are found to exist as lamellar structured eutectic mixture of $Mg_{12}La$ and α -Mg or as other secondary phases. There are different types of phases that may form in Mg-La alloys, such as $Mg_{12}La$, $Mg_{17}La_2$, or Mg_2La phases [7]. It remains unclear which exact phase will form under different solidification conditions. The formation of $Mg_{12}La$ as opposed to $Mg_{17}La_2$ is subject to a debate [8,9].

In view of the respective ability of Ce and La to enhance ductility and strength, this research work was designed to harness their respective abilities by alloying them together with Mg as the principal element. The analysis of microstructure and mechanical properties was undertaken to validate their cumulative ability to develop a superior ternary alloy.

2. Materials and Methods

In this study, Mg turnings of >99.9% purity were used as matrix material. They were supplied by ACROS Organics, New Jersey, USA. The Rare Earths were added in the form of master alloys (Mg-30%RE) with >99% purity obtained from Sunrelier Metal Co. Limited, Pudong, Shanghai, China. Mg-4La-0.4Ce alloy was synthesized using the Disintegrated Melt Deposition technique [6]. The ingot obtained from casting was machined and soaked at 400 °C for 1 hour in a constant temperature furnace before extrusion. Hot extrusion was performed using a 150-ton hydraulic press at 350 °C die temperature with an extrusion ratio of 20.25:1. Rods of 8 mm diameter were produced. Specimen were taken from the extruded rod for various characterization studies.

Micro-hardness tests were conducted on flat and metallographically polished specimen in accordance with ASTM (American Society for Testing and Materials) standard E384-16 with an indenting load of 25 gramforce (gf) for a dwell time of 15 s and were recorded in Vickers Hardness (HV). Twenty indentations were made for each sample. The tensile tests were carried out in accordance with ASTM test standard E8/E8 M-16a. Extruded rods were machined to dog bone shape with 25 mm gauge length and 5 mm gauge diameter. Material Test System (MTS 810) (Eden Prairie, MN, USA), with a clip-on type extensometer and a strain rate of $1.67 \times 10^{-4} \text{ s}^{-1}$, was used to conduct tests. The compressive tests were carried out along the extrusion direction, in accordance with ASTM test method E9-09 on the MTS 810 testing machine at ambient temperature, using a strain rate of $1.67 \times 10^{-4} \text{ s}^{-1}$. A minimum of three samples were tested to ensure consistent values during tensile and compressive testing. To investigate the microscopic features and fracture mechanisms of the samples, JEOL JSM-6010 PLUS/LV Scanning Electron Microscope with EDS (Jeol USA Inc., Peabody, MA, USA) was used. X-ray diffraction was performed to identify phases by matching the Bragg angles with the standard values of Mg, Ce and La related possible phases. The polished specimen were etched using the etchant: 0.7 mL H_3PO_4 , 4 g picric acid and 100 mL ethanol (45%). Leica DM2500 M metallographic optical microscope (Leica Microsystems (SEA) Pte Ltd., Singapore, Singapore) was used to analyse the grain size of samples.

3. Results

3.1. Microstructural Characterization

To understand the phase distribution as well as the structure, X-ray diffraction (XRD) studies were done. XRD results confirm the presence of peaks that correspond to the secondary phase $Mg_{17}La_2$ in Mg-4La-0.4Ce (see Figure 1). Optical microscopy investigations revealed nearly equiaxed grain morphology of Mg, Mg-0.4Ce and Mg-4La-0.4Ce (see Figure 2a,b). The grain size of Mg-4La-0.4Ce ($1.3 \pm 0.2 \mu\text{m}$) was significantly lower compared to both Mg ($25 \pm 4 \mu\text{m}$) and Mg-0.4Ce ($4 \pm 1 \mu\text{m}$) [10].

This demonstrates the capability of La to refine grain size through the formation of secondary phases. The results of SEM imaging further confirmed the presence of secondary phases in the alloy (see Figure 2c,d). The secondary phases ($Mg_{17}La_2$) were segregated and distributed discontinuously across grains (see Figure 2c,d). $Mg_{17}La_2$ phase had a size of about $1 \pm 0.5 \mu m$ unlike $Mg_{17}Ce_2$ phase in Mg-0.4Ce alloy whose size was much lower than $1 \mu m$ [6]. Further, it is also interesting to note that the $Mg_{17}La_2$ secondary phases with a much higher volume fraction of ~ 0.46 as compared to $Mg_{17}Ce_2$ phase in Mg-0.4Ce alloy (vol. fraction of ~ 0.04), were distributed throughout the matrix. It has been established before that secondary phases serve as pinning points during recrystallization and hinder grain growth resulting in the effective reduction of grain size [4]. Although the formation of other phases is predicted based on the phase diagram, other secondary phases were not detected, presumably due to their minimal presence arising from lower alloying concentration of La and Ce in the ternary alloy developed in this study.

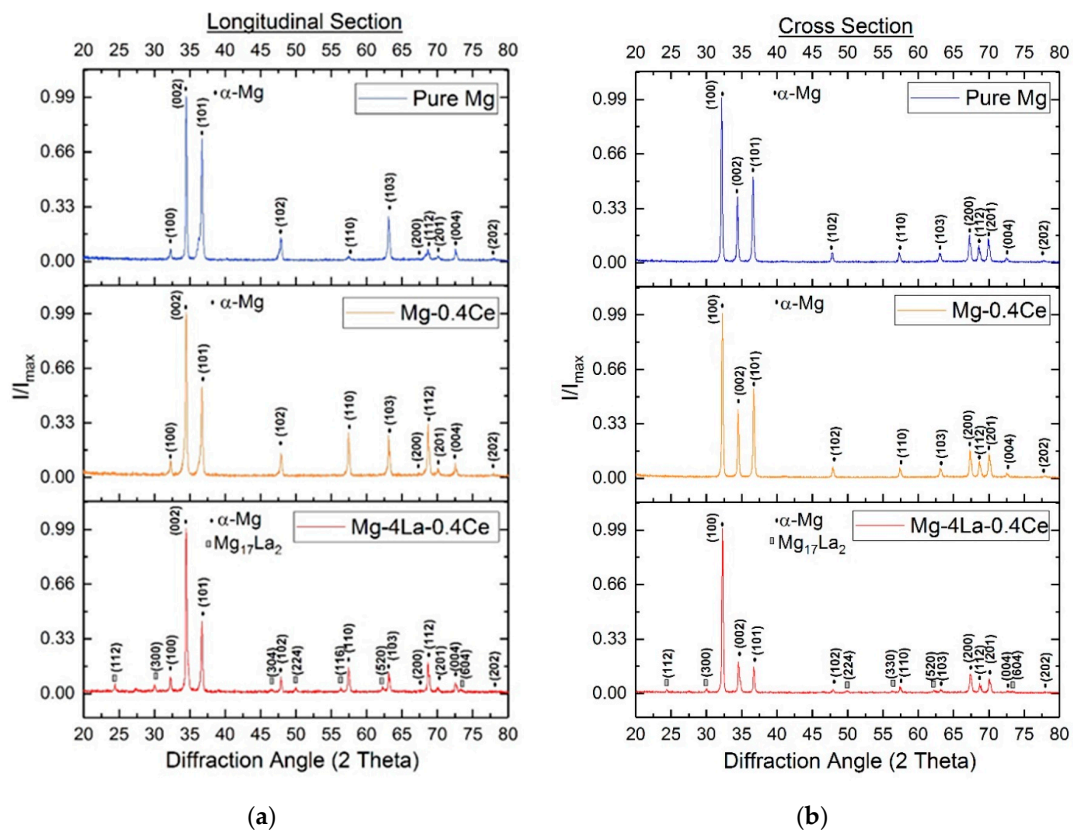


Figure 1. XRD results of extruded samples along (a) cross section and (b) longitudinal direction.

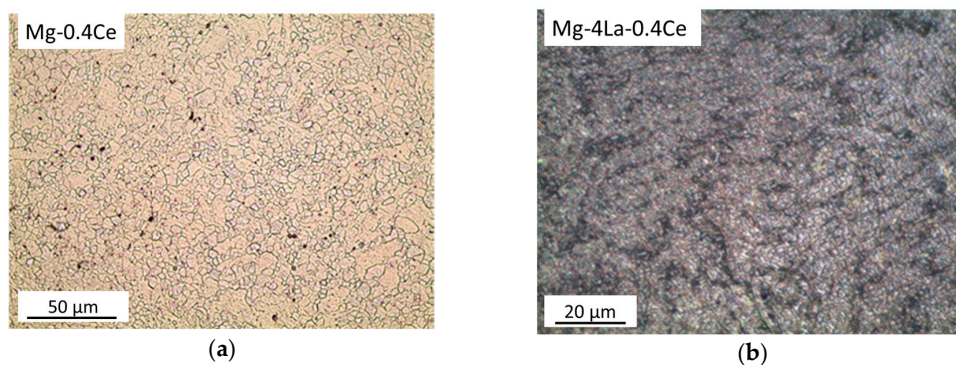


Figure 2. Cont.

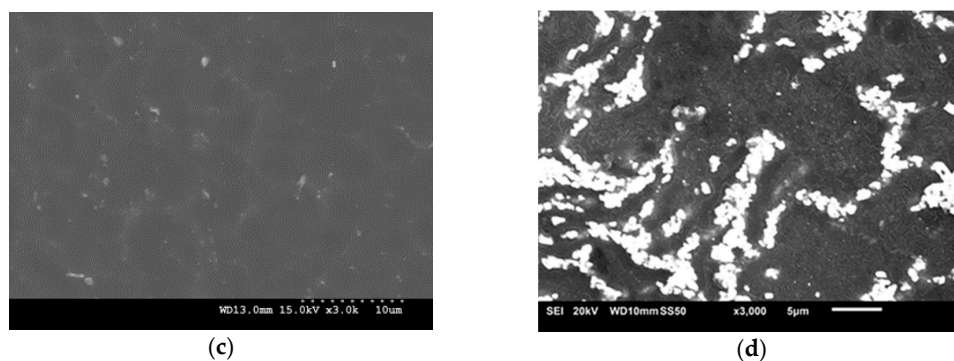


Figure 2. Representative micrographs showing grain boundaries and grain morphology of (a) Mg-0.4Ce and (b) Mg-4La-0.4Ce alloys; Representative micrographs showing the phases and distribution of phases in the (c) Mg-0.4Ce and (d) Mg-4La-0.4Ce alloys.

3.2. Mechanical Characterization

Microhardness measurements on Mg-4La-0.4Ce show that it has a microhardness of 107 HV. It is harder than pure Mg by 62% and Mg-0.4Ce by 24%. This improvement in the microhardness is attributed to the refined grain size and presence of large fraction of hard secondary phases. The microhardness, tensile, and compressive test results are summarized in Table 1. Under tensile loading, Mg-4La-0.4Ce exhibits 241% increase in tensile yield strength and 102% increase in ultimate tensile strength compared to pure Mg. Under compressive loading, its yield strength is 195% higher and its ultimate strength is 42% higher compared to pure Mg. Irrespective of the significant increase in tensile strengths, tensile ductility of the ternary alloy remained at 19%, which is about an increase of ~36% over that of pure Mg. Under compressive loading, ductility reduced by 30% when compared to pure Mg and was ~16% which is quite similar to its tensile ductility. Compared with the as-extruded commercial Mg-RE alloy WE43 [11], Mg-4La-0.4Ce with less weight percentage of expensive RE demonstrates to be more cost effective and displayed 13% increase in tensile yield strength as well as 76% increase in ductility (see Figure 3). The function of Ce as a ductility enhancer is further justified by the comparison of ductility between Mg-4La-0.4Ce and other La rich Mg alloys without Ce addition. Mg-4La-0.4Ce demonstrates 1800%, 171% and 138% increase in ductility in comparison with Mg-3.44La, Mg-4Al-4La and Mg-4.2La-0.5Zr alloys respectively [7,12,13].

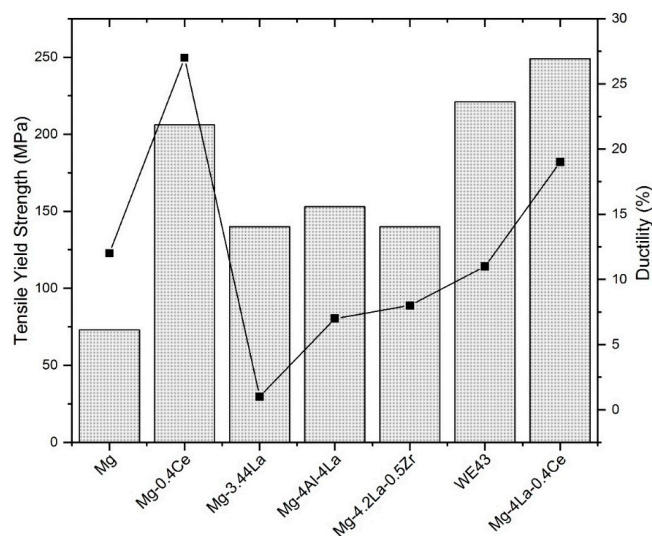


Figure 3. Tensile yield strength and ductility of extruded Mg-4La-0.4Ce alloy in comparison to pure Mg, Mg-0.4Ce, WE43 and other La rich alloys.

Table 1. Mechanical characteristics of pure Mg, Mg-0.4Ce and Mg-4La-0.4Ce.

Material	Micro-Hardness	0.2% Offset Yield Strength (MPa)		Ultimate Strength (MPa)		Fracture Strain (%)		Energy Absorbed (MJ/M ³)	
		Tensile	Compressive	Tensile	Compressive	Tensile	Compressive	Tensile	Compressive
Pure Mg	66 ± 3.3	73 ± 9	66 ± 4	130 ± 21	309 ± 14	14 ± 5.2	23 ± 3.5	15 ± 8.2	41 ± 3.9
Mg-0.4Ce	86 ± 3.1	206 ± 8	144 ± 10	223 ± 6	411 ± 5	27 ± 2.3	25 ± 1.9	56 ± 3.2	62 ± 2.7
Mg-4La-0.4Ce	107 ± 2.0 (+62%)	249 ± 2 (+241%)	195 ± 11 (+195%)	263 ± 1 (+102%)	438 ± 5 (+42%)	19 ± 2.2 (+36%)	16 ± 0.6 (−30%)	49 ± 5.8 (+227%)	43 ± 1.4 (+5%)

± Indicate the increase/decrease with respect to the same property of pure Mg.

4. Discussion

4.1. Tensile Deformation Behavior

The Mg-4La-0.4Ce alloy shows an increased tensile and compressive strength compared to both the Mg and Mg-0.4Ce alloys. There are two possible strengthening mechanisms: (1) Hall-Petch strengthening arising from enhanced grain boundary area that resists the easy movement of dislocations; and (2) precipitation strengthening due to the presence of secondary phases which act as obstacles to dislocation motion. It may be noted that, due to the limited solubility of La in Mg, solid solution strengthening is not effective in the alloy at room temperature.

The Hall-Petch relation [14] defines the relationship between grain size and the yield stress as follows: $\sigma(d) = \sigma_0 + kd^{-1/2}$ where σ is the 0.2% yield stress, d is the grain size, k is the strengthening coefficient and σ_0 is material constant. The grain size of Mg-4La-0.4Ce is around 1.3 μm which is much smaller (−68%) than that of Mg-0.4Ce (4 μm). This substantiates the previously reported result by Stanford et al. that La is one of the most effective grain refiners per atomic percent, as compared to other alloying elements like Al, Sn, Ca and Gd [3]. As a result, the tensile strength of Mg-4La-0.4Ce is much higher than that of the Mg and Mg-0.4Ce alloys. In addition, there is a considerably higher density of secondary phases in Mg-4La-0.4Ce compared to Mg-0.4Ce. The strength of Mg alloys with La addition increases due to the additional presence of secondary phases [10]. The presence of secondary phases impedes the motion of moving dislocations leading to an increase in strength as per classical theory of precipitation strengthening [15]. Therefore, the primary deformation mechanisms under tension (slip) are suppressed due to the presence of large volume of secondary phases [16]. This leads to a greater effect of precipitation hardening and thus a much higher tensile yield strength is exhibited by Mg-4La-0.4Ce. Further, due to its finer grain size, slip flexibility is promoted, which implies a more homogeneous and uniform plasticity across the entire polycrystal. Thus, the enhanced ductility in comparison to pure Mg is achieved. However, this concept cannot be used in comparison to Mg-0.4Ce alloy as the precipitate fraction in Mg-4La-0.4Ce is much higher, obstructing a higher ductility as compared to Mg-0.4Ce alloy.

Fracture studies were performed to investigate the mode of failure. Figure 4 shows the fractographs of samples after tensile failure. A pure Mg fractograph (Figure 4a) shows the presence of cleavage steps indicative of brittle failure. The fractograph of Mg-0.4Ce alloy (Figure 4b) displays the presence of dimples indicative of ductile failure (tensile elongation: 27%). The fracture morphology of Mg-4La-0.4Ce (Figure 4c) reveals minimal presence of cleavage steps and significant evidence of plastic deformation (tensile ductility = 19%) [17]. Comparing the fractographs of Mg, Mg-0.4Ce alloy and ternary Mg-4La-0.4Ce alloy, it can be ascertained that Mg-4La-0.4Ce featured a larger fraction of dimples as compared to Mg and a larger fraction of cleavage steps as compared to the Mg-0.4Ce alloy, which is substantiated by the results of its tensile ductility that ranges between the two monolithic materials.

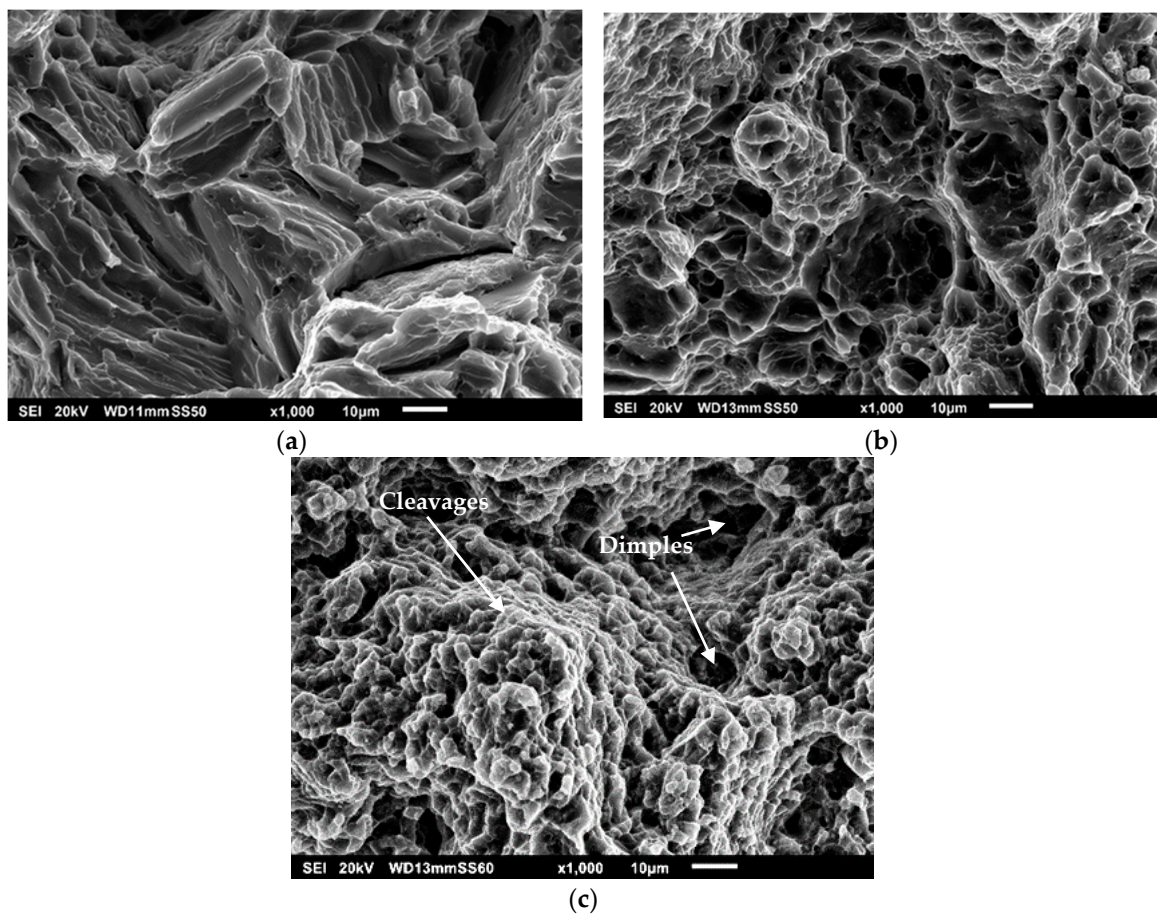


Figure 4. Tensile fractographs of: (a) Mg; (b) Mg-0.4Ce alloy and (c) Mg-4La-0.4Ce alloy.

4.2. Compressive Deformation Behavior

The compressive yield strength of Mg-4La-0.4Ce was higher than that of pure Mg and the Mg-0.4Ce alloy (Table 1). Under compression along the extrusion direction of Mg alloys, deformation occurs by twin followed by slip [18]. To investigate the role of twinning under compression, the compressive tests were stopped just at the yield point, after the yield point and after attaining ultimate strength (see Figure 5) and the samples were studied to understand the deformation. The following were observed: there were no twins found in the sample just at the yield point (See Figure 6a). However, twins have been found after allowing the material to strain to a considerable extent after the yield point (See Figure 6b) as well as at ultimate compressive strength (See Figure 6c). This shows the dominance of twinning at the initial stage of plastic deformation under compression which corresponds to the plateau in the stress-strain curve (See Figure 5) [19]. Further deformation along c-axis after the initial stage is aided by shear mode of deformation. Quantification of the twin fraction was done as given in Figure 5 and it is seen that the twin fraction after yield point in Mg-4La-0.4Ce alloy (~ 0.08) is lower than that of Mg-0.4Ce alloy (~ 0.24). Further, with increase in the stress, the twinning was propagated in both the alloys; however, the twin fraction was still lower for the Mg-4La-0.4Ce alloy (~ 0.29) as compared to the Mg-0.4Ce alloy (~ 0.54) at UCS. This is due to the suppression of deformation twinning in alloys with smaller grains as compared to alloys with larger grain size [16]. Furthermore, the presence of secondary phases would suppress both twin and slip [20]. Since Mg-4La-0.4Ce has a combination of both: smaller grain size and larger amount of secondary phases, the effect of suppression of twinning is greater compared to Mg-0.4Ce alloy (the deformation studies of the Mg-0.4Ce alloy are given in reference [6]). However, this effect comes at the expense of ductility. As a result, the elongation to failure in Mg-4La-0.4Ce (16%) is less than that of Mg-0.4Ce (25%). In addition to the role of grain size

and precipitation in the activation energy of twinning, texture effect also influences the deformation twinning. Alloys with weakened basal texture, especially the RE-texture component, would have grain alignment favoring both slip and deformation twinning [3]. In order to understand the texture effect, XRD results of extruded samples along longitudinal section were analyzed (see Figure 1b), as a study on the cross section of the samples leads to a lower intensity of the basal planes if the material exhibits a strong basal texture. The diffraction angle, 2 theta, at 32°, 34°, and 36° corresponds to prismatic {100}, basal {002} and pyramidal {101} planes of hexagonally close packed (HCP) magnesium crystal respectively [21]. The ratio of intensity (I/I_{max}) at 32°, 34°, and 36° to the maximum intensity is listed in Table 2. The highest ratio was found at 34° for all the three alloys, which also indicates that Mg-4La-0.4Ce still has a basal dominant texture, typical of extruded alloys. This I/I_{max} of Mg-4La-0.4Ce is higher than that of pure Mg, indicating a comparatively stronger basal texture. This texture effect further enhances its strength and gives rise to a lower ductility.

To confirm the mode of failure under compression, fracture studies were performed. Under compressive loading, fracture surfaces were at approximately 45 degrees, with respect to the compression testing direction. Shear bands were observed (see Figure 6d), which is an indication of shear mode of failure.

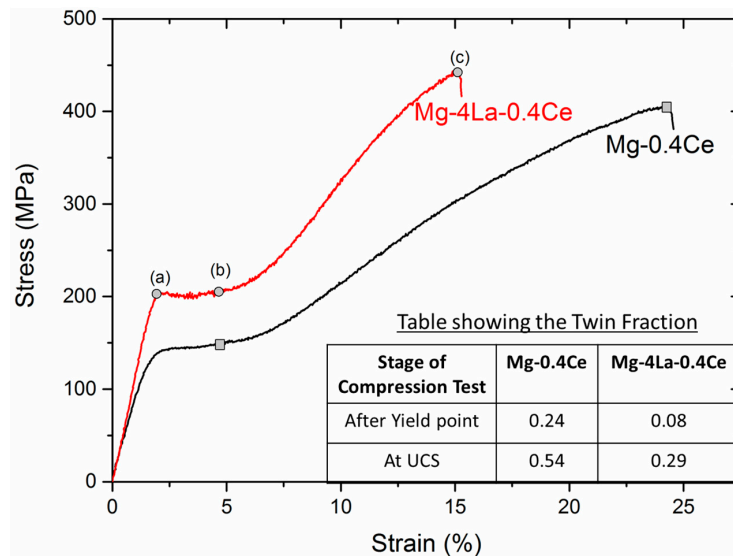


Figure 5. Results from compressive test: stress-strain curve of Mg-4La-0.4Ce showing the points where tests were stopped at: (a) yield point; (b) after yield point and (c) at ultimate compressive yield strength.

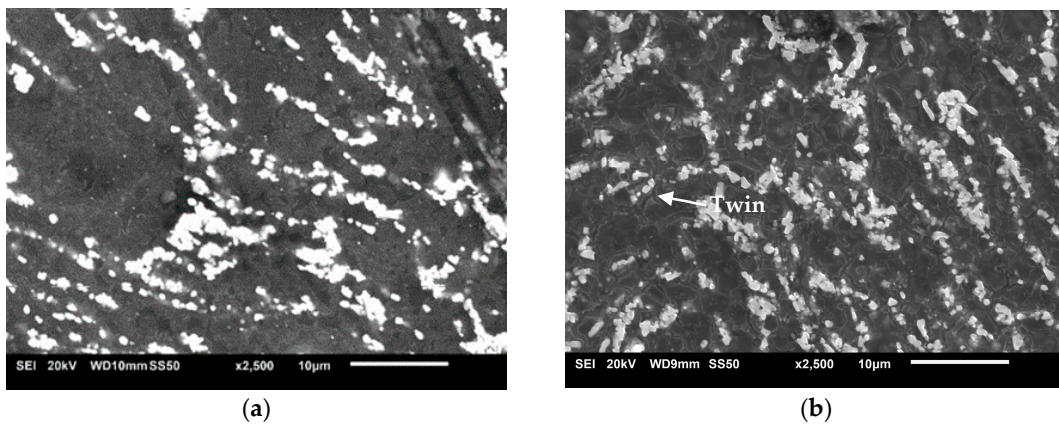


Figure 6. Cont.

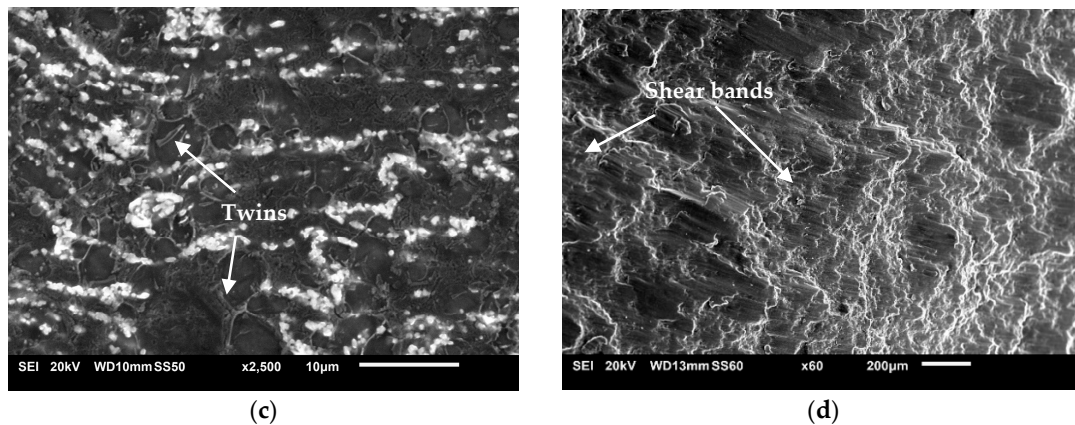


Figure 6. Microstructure of deformed Mg-4La-0.4Ce after compression test at: (a) yield point; (b) after yield point; (c) at ultimate yield strength and (d) after fracture.

Table 2. Ratio of intensity to the maximum intensity at 32° ($\{100\}$ prismatic plane), 34° ($\{002\}$ basal plane) and 36° ($\{101\}$ pyramidal plane).

Composition	I/I_{\max} at 32°	I/I_{\max} at 34°	I/I_{\max} at 36°
Mg	0.027	0.02703	0.0676
Mg-0.4Ce	0.04	0.1036	0.04
Mg-4La-0.4Ce	0.0197	0.0333	0.0258

4.3. Tension-Compression Yield Asymmetry

Mg alloys usually demonstrate very different plastic flow characteristics under tension and compression due to the strong basal texture and high c/a ratio of Mg [20]. The poor compressive yield strength associated with yield asymmetry limits the applications of Mg alloys [22]. The yield asymmetry of Mg alloys can be characterized by calculating the ratio of compressive yield strength (CYS) to tensile yield strength (TYS). Usually this ratio is well below 1 because typical Mg alloys have compressive yield strengths much lower than their tensile yield strengths [20]. The ratio of CYS/TYS for Mg, Mg-0.4Ce and Mg-4La-0.4Ce is shown in the Table 3. Mg-4La-0.4Ce showed a ratio of 0.78 in comparison with Mg-0.4Ce whose ratio is 0.7. Pure Mg, with the largest grain size, has poor CYS and TYS , hence its asymmetry is not very pronounced. Addition of Ce refines the grain size, therefore, enhancing the TYS and CYS greatly. However, due to the pronounced difference in the deformation mechanisms, there exists a higher difference between TYS and CYS . This is due to the difference between the activation energy of twinning and slip. Results revealed that the presence of La assisted in the improvement of yield symmetry of Mg-0.4Ce alloy. Despite finer grain size in the ternary alloy, the yield symmetry improved, as compared to the Mg-0.4Ce alloy. This is due to the stark difference in the strength of texture. From Table 2, the I/I_{\max} ratio at 34° is only 0.0333 for Mg-4La-0.4Ce while it is 0.1 for Mg-0.4Ce (stronger basal texture). This is an indication of the higher energy of activation for basal slip in Mg-0.4Ce alloy compared to Mg-4La-0.4Ce alloy. Further, the beneficial effect of the presence of larger volume of secondary phases in Mg-4La-0.4Ce which assisted in increasing the compressive yield strength, are constitutively responsible for reducing tension–compression yield asymmetry.

Table 3. The CYS , TYS and CYS/TYS for extruded Mg, Mg-0.4Ce and Mg-4La-0.4Ce alloys.

Composition	CYS (MPa)	TYS (MPa)	CYS/TYS
Mg	66	73	0.90
Mg-0.4Ce	144	206	0.70
Mg-4La-0.4Ce	195	249	0.78

5. Conclusions

Ternary Mg-4La-0.4Ce alloy was successfully synthesized using disintegrated melt deposition technique. The synergistic effect of ductility enhancer Ce and strength enhancer La on Mg was investigated. The following conclusions are drawn from this study:

1. Mg-4La-0.4Ce exhibited 241% and 21% increase in tensile yield strength and 102% and 18% increase in ultimate tensile strength, when compared to pure Mg and Mg-0.4Ce, respectively. Tensile ductility of Mg-4La-0.4Ce remained at ~19%.
2. Mg-4La-0.4Ce alloy exhibited 195% and 35% increase in compressive yield strength and 42% and 7% increase in ultimate compressive strength compared to Mg and Mg-0.4Ce, respectively. Compressive ductility was retained at ~16%.
3. A reduced tension–compression yield asymmetry was found in Mg-4La-0.4Ce alloy when compared to Mg-0.4Ce alloy.
4. Presence of La helped in refinement of the grain size (1.3 μm) when compared to Mg (25 μm) and Mg-0.4Ce alloy (4 μm).
5. The improvement in micro-hardness by ~62% and ~21% over that of Mg and Mg-0.4Ce alloy is attributed to reduction in grain size and significant presence of secondary phases in Mg-4La-0.4Ce.
6. Suppression of twinning, to an extent, due to presence of refined grains, large fraction of secondary phases and basal dominant texture are the main reason for improved compressive strength of Mg-4La-0.4Ce alloy.

Acknowledgments: The authors thank Juraimi Bin Madon for the help with extrusion. One of the authors, Yang Wei, expresses his gratitude to Sembcorp Industries Ltd for the full scholarship of his undergraduate study. The authors also gratefully acknowledge Ministry of Education Academic Research Funding (WBS# R-265-000-498-112) for the financial support.

Author Contributions: Manoj Gupta and Sravya Tekumalla conceived and designed the experiments; Yang Wei performed experiments; Yang Wei and Sravya Tekumalla analyzed the data; Yang Wei, Sravya Tekumalla and Manoj Gupta wrote the paper.

Conflicts of Interest: The authors declare no conflict of interest. The founding sponsors had no role in the design of the study; in the collection, analyses, or interpretation of data; in the writing of the manuscript, and in the decision to publish the results.

References

1. Chino, Y.; Kado, M.; Mabuchi, M. Compressive Deformation Behavior at Room Temperature–773 K in Mg-0.2 mass % (0.035 at %) Ce alloy. *Acta Mater.* **2008**, *56*, 387–394. [[CrossRef](#)]
2. Solanki, K.; Moitra, A.; Bhatia, M. Effect of Substituted Aluminum in Magnesium Tension Twin. In *Magnesium Technology 2011*; Sillekens, W., Agnew, S., Neelameggham, N., Mathaudhu, S., Eds.; Springer International Publishing: Hoboken, NJ, USA, 2011; pp. 325–329.
3. Stanford, N.; Barnett, M. The origin of “rare earth” texture development in extruded Mg-based alloys and its effect on tensile ductility. *Mater. Sci. Eng. A* **2008**, *496*, 399–408. [[CrossRef](#)]
4. Mishra, R.K.; Gupta, A.K.; Rao, P.R.; Sachdev, A.K.; Kumar, A.M.; Luo, A.A. Influence of cerium on the texture and ductility of magnesium extrusions. *Scr. Mater.* **2008**, *59*, 562–565. [[CrossRef](#)]
5. Chino, Y.; Kado, M.; Mabuchi, M. Enhancement of tensile ductility and stretch formability of magnesium by addition of 0.2 wt % (0.035 at.%) Ce. *Mater. Sci. Eng. A* **2008**, *494*, 343–349. [[CrossRef](#)]
6. Tekumalla, S.; Seetharaman, S.; Bau, N.Q.; Wong, W.L.E.; Goh, C.S.; Shabadi, R.; Gupta, M. Influence of Cerium on the Deformation and Corrosion of Magnesium. *J. Eng. Mater. Technol.* **2016**, *138*, 031011. [[CrossRef](#)]
7. Chia, T.L.; Easton, M.A.; Zhu, S.M.; Gibson, M.A.; Birbilis, N.; Nie, J.F. The effect of alloy composition on the microstructure and tensile properties of binary Mg-rare earth alloys. *Intermetallics* **2009**, *17*, 481–490. [[CrossRef](#)]

8. Wang, Y.F.; Zhang, W.B.; Wang, Z.Z.; Deng, Y.H.; Yu, N.; Tang, B.Y.; Zeng, X.Q.; Ding, W.J. First-principles study of structural stabilities and electronic characteristics of Mg-La intermetallic compounds. *Comput. Mater. Sci.* **2007**, *41*, 78–85. [[CrossRef](#)]
9. Tamura, Y.; Murakami, M.; Soda, H.; McLean, A. Role of Lanthanum in Grain Refinement and Tensile Properties of Cast Mg-La-Zr Alloys. *Mater. Trans.* **2013**, *54*, 745–754. [[CrossRef](#)]
10. Tekumalla, S.; Tekumalla, S.; Seetharaman, S.; Almajid, A.; Gupta, M. Mechanical properties of magnesium-rare earth alloy systems: A review. *Metals* **2014**, *5*, 1–39. [[CrossRef](#)]
11. Zhang, X.; Yuan, G.; Mao, L.; Niu, J.; Ding, W. Biocorrosion properties of as-extruded Mg-Nd-Zn-Zr alloy compared with commercial AZ31 and WE43 alloys. *Mater. Lett.* **2012**, *66*, 209–211. [[CrossRef](#)]
12. Yang, Q.; Meng, J.; Tian, Z.; Qiu, X.; Meng, F. Microstructures and tensile properties of Mg-4Al-4La-0.4Mn-xB ($x = 0, 0.01, 0.02, 0.03$) alloy. *J. Alloys Compd.* **2013**, *572*, 129–136. [[CrossRef](#)]
13. Tachibanaki, J.; Tamura, Y.; Soda, H.; McLEAN, A. Ductility and Deformation Structure of Mg-La-Zr Alloys. *J. Jpn. Soc. Technol. Plast.* **2015**, *56*, 60–65. [[CrossRef](#)]
14. Petch, N.J. The cleavage strength of polycrystals. *J. Iron Steel Inst.* **1953**, *174*, 25–28.
15. Martin, J.W. *Precipitation Hardening: Theory and Applications*; Butterworth-Heinemann: Oxford, UK, 2012.
16. Yoo, M. Slip, twinning, and fracture in hexagonal close-packed metals. *Metall. Trans. A* **1981**, *12*, 409–418. [[CrossRef](#)]
17. Hertzberg, R.W.; Vinci, R.P.; Hertzberg, J.L. *Deformation and Fracture Mechanics of Engineering Materials*, 5th ed.; John Wiley and Sons: Hoboken, NJ, USA, 2012.
18. Zhang, D.; Jiang, L.; Zheng, B.; Schornung, J.M.; Mshajan, S.; Lavernia, E.J. Deformation Twinning (Update). *Ref. Modul. Mater. Sci. Eng.* **2016**, 1–24.
19. Chen, Y.; Tekumalla, S.; Guo, Y.B.; Gupta, M. Introducing Mg-4Zn-3Gd-1Ca/ZnO nanocomposite with compressive strengths matching/exceeding that of mild steel. *Sci. Rep.* **2016**, *6*, 32395. [[CrossRef](#)] [[PubMed](#)]
20. Zhang, D.; Haiming, W.; Kumar, M.A.; Chen, F.; Zhang, L.; Beyerlein, I.; Schoenung, J.M.; Mshajan, S.; Lavernia, E.J. Yield symmetry and reduced strength differential in Mg-2.5 Y alloy. *Acta Mater.* **2016**, *120*, 75–85. [[CrossRef](#)]
21. Rashad, M.; Pan, F.; Hu, H.; Asif, M.; Hussain, A.; She, J. Enhanced tensile properties of magnesium composites reinforced with graphene nanoplatelets. *Mater. Sci. Eng. A* **2015**, *630*, 36–44. [[CrossRef](#)]
22. Ball, E.A.; Prangnell, P.B. Tensile-compressive yield asymmetries in high strength wrought magnesium alloys. *Scr. Metall. Mater.* **1994**, *31*, 111–116. [[CrossRef](#)]



© 2017 by the authors. Licensee MDPI, Basel, Switzerland. This article is an open access article distributed under the terms and conditions of the Creative Commons Attribution (CC BY) license (<http://creativecommons.org/licenses/by/4.0/>).